Egyptian Journal of Aquatic Research 51 (2025) 505–516

Contents lists available at ScienceDirect

Egyptian Journal of Aquatic Research

journal homepage: www.elsevier.com/locate/ejar

Full length article

Microphytoplankton community structure in the Gulf of Aqaba and northern Red Sea

Mohsen M. El-Sherbiny [a,*], Zaki M. Al-Hasawi [b], Mohamed E. EL-Hefnawy [c]

[a] Department of Marine Biology, Faculty of Marine Science, King Abdulaziz University, Jeddah 21589, Saudi Arabia
[b] Biological Sciences Department, Faculty of Science and Arts, King Abdulaziz University, Rabigh 21911, Saudi Arabia
[c] Department of Marine Chemistry, Faculty of Marine Science, King Abdulaziz University, Jeddah 21589, Saudi Arabia

ARTICLE INFO

Keywords:
Microphytoplankton
Diversity
Biomass nutrients
Gulf of Aqaba
Northern Red Sea

ABSTRACT

Phytoplankton assemblages and species richness were examined with respect to physico-chemical parameters in Gulf of Aqaba (GoA) and northern Red Sea (NRS) during early spring (March 2018). Three stations were selected for the current study in each of the GoA and NRS. Water temperature was significantly lower ($p < 0.05$) and salinity higher ($p < 0.01$) in the GoA than in the NRS. Ammonia varied spatially, whereas nitrate, nitrite, and silicate showed vertical gradients. In contrast, phosphate concentration remained uniform. Chlorophyll-*a* was stable in the NRS but declined from south to north in the GoA. Phytoplankton density in GoA increased from station 1 to 3, whereas NRS densities exhibited minimal change. Chlorophyll-*a* and phytoplankton density were significantly correlated with temperature ($r = 0.57$, $p < 0.01$), while community structure varied spatially as indicated by MDS anlysis. Diatoms dominated some stations, whereas dinoflagellates were numerically dominant in others. Among the 179 phytoplankton species recorded, dinoflagellates accounted for 100 (of which 27 were heterotrophic), diatoms 78, and cyanophytes one. Diatoms (including *Chaetoceros* spp. and *Rhizosolenia* spp.) and dinoflagellates (such as *Tripos* spp. and *Protoperidinium* spp.) exhibited greater diversity. Three diatom species and seven dinoflagellate species known to cause severe algal blooms worldwide were also recorded from the region.

Introduction

The Red Sea is a semi-enclosed tropical basin that is commonly divided into three main regions based on hydrographic and ecological features, namely the northern Red Sea (NRS), central Red Sea, and southern Red Sea. The NRS includes the Gulf of Aqaba (GoA) and extends southward to approximately 20°N, whereas the central Red Sea spans from about 20°N to 16°N, and the southern Red Sea stretches from 16°N to the Bab el Mandeb Strait (Raitsos et al., 2013; Rasul et al., 2018). Such a classification is essential for understanding regional variability in oceanographic conditions and biological productivity. The Red Sea is a predominantly oligotrophic system due to limited availability of inorganic nutrients that are necessary for sustaining photosynthetic activity (Morcos, 1970). The nutrient content in the Red Sea is primarily influenced by the inflow of nutrient-enriched Indian Ocean water via the Gulf of Aden (Zhan et al., 2014; Qurban et al., 2017; Kürten et al., 2019). Additionally, winter mixing also influences nutrient availability by promoting the ascent of deeper, nutrient-laden waters to the surface (Labiosa et al., 2003; Sofianos & Johns, 2003). Latitudinal disparity in nutrient availability creates a gradient, with concentrations decreasing from south to north (e.g. Kürten et al., 2015; Kheireddine et al., 2017). Conditions such as hot, arid climate and elevated water column salinity create unfavorable conditions for the proliferation of marine phytoplankton (Sofianos, Johns, & Murray, 2002). The southern Red Sea supports the proliferation of phytoplankton across all seasons due to its high natural nutrient content (Dreano et al., 2016; Pearman et al., 2017). In contrast, primary productivity in the NRS is entirely dependent on winter because nutrient concentrations are elevated in winter compared to the other seasons (Lindell & Post, 1995). During summers, NRS exhibits extreme oligotrophic system owing to the presence of a stratified water column (e.g. Racault et al., 2015; Devassy et al., 2017).

The GoA is the northeastern extension of the Red Sea and exhibits similar summer water column characteristics to those of NRS (Manasrah et al., 2004; Acker et al., 2008). During summer, both these regions experience strong stratification, which limits surface nutrient

* Corresponding author.
E-mail address: ooomar@kau.edu.sa (M.M. El-Sherbiny).

https://doi.org/10.1016/j.ejar.2025.09.001
Received 25 June 2025; Received in revised form 2 September 2025; Accepted 3 September 2025
Available online 4 October 2025

replenishment and significantly reduces primary productivity (Grossart & Simon, 2002; Reiss & Hottinger, 2012; Laiolo et al., 2014; Şahin et al., 2022; Berman & Gildor, 2022; Nassar & Fahmy, 2023). In contrast, winter mixing facilitates upward transport of nutrients, enhancing phytoplankton growth that can extend into the spring season (Stambler, 2005). GoA in the summer season exhibit weak thermocline, highly oxygenated surface waters, and minimal availability of nutrients (Klinker et al., 1978). Similar to the phenomenon in the NRS, deep water mixing results in the movement of nutrients upward from deep layers to the surface in the winter period that subsequently increase the rate of primary production. Comparatively higher primary production in winter period continues into the spring season for both the regions, suggesting that regenerated winter nutrients may sustain elevated phytoplankton biomass in spring, as reported by recent remote sensing studies (Acker et al., 2008; Racault et al., 2015). Most studies conducted in the region have primarily focused on the picophytoplankton dynamics (Lindell & Post, 1995; Stambler, 2005), whereas only a few focused on microphytoplankton assemblages of GoA (e.g. Sommer et al., 2002; Al-Najjar et al., 2007; Nassar, 2007; Iluz et al., 2009; Madkour et al., 2010) and NRS (Devassy et al., 2017). The composition and diversity of phytoplankton populations in the GoA displays pronounced seasonal variability, with ultraphytoplankton predominating in spring and summer, whereas larger phytoplankton groups become more dominant during winter (Lindell & Post, 1995). Normally, phytoplankton in both the NRS and GoA is dominated mainly by ultraphytoplankton of size < 8 μm and the medium-sized phytoplankton or microphytoplankton (> 20 μm) is scarce (Lindell & Post, 1995; Sommer, 2000).

In the present study, we aimed to compare the spring microphytoplankton dynamics in the NRS and GoA and provide a detailed taxonomical insight into the microphytoplankton community of both regions. To our knowledge, our study can be considered as new record, which focuses on the vertical distribution of phytoplankton biomass and distribution during the spring season, where the remnants of inorganic nutrients that generated through the winter convection still prevails.

Materials and methods

Sampling location

A total of six sampling stations, three each in GoA and NRS, were selected to compare microphytoplankton dynamics during early spring (17–23 March 2018) (Fig. 1).

Sampling and analysis

Field sampling from all the stations was carried out during day time (between 10:00–12:00) during March 17–23, 2018. Temperature, salinity, and dissolved oxygen profiles were obtained to a depth of 200 m using a pre-calibrated CTD profiler (SBE 25 plus, Seabird Electronics).

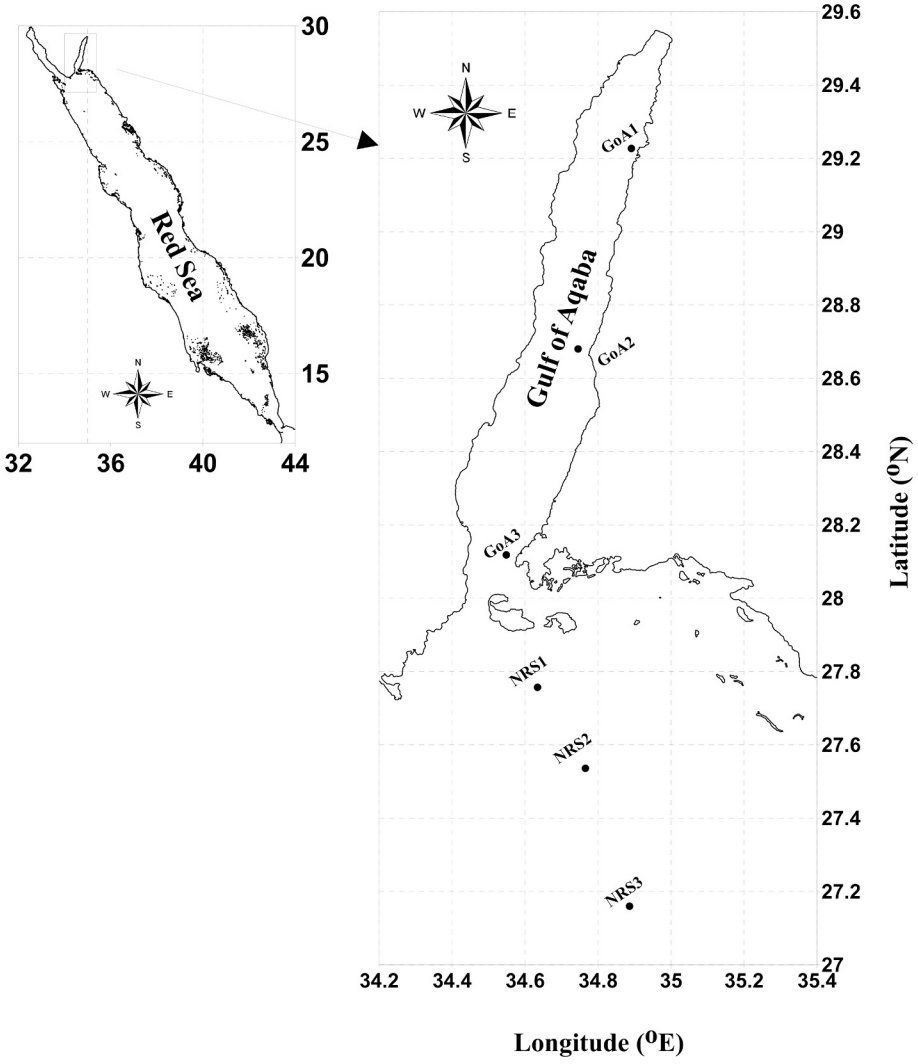

Fig. 1. Map showing different sampling stations.

Water samples for chlorophyll-*a* and nutrient analysis were collected from six discrete depths (5, 25, 50, deep chlorophyll maximum (DCM), 100, and 200 m) using a Niskin rosette sampler (SBE 33). DCM was identified in situ using CTD fluorescence data and typically ranged between 60–70 m. Chlorophyll-*a* was determined for each depth using 4–5 L of seawater and subjecting it to filtration via Whatman GF/F filter paper with 0.7 μm pores using a vacuum pump. Inorganic nutrient concentrations for each depth was determined using 500 ml of seawater subjected to filtration using a nucleopore membrane filter (Whatman) of pore size 0.2 μm, with the filtered water collected in clean Nalgene bottles.

Filter papers (for chlorophyll-*a*) and the corresponding filtrates (for nutrient analysis) were stored at − 80 °C until laboratory analysis. Phytoplankton samples from each station were obtained by vertical haul from a depth of 120 m to the surface using a Hydrobios plankton net with a 20 μm mesh. A Hydrobios flowmeter with back-run stop capability was attached to the net opening before each tow to quantify the volume of water filtered. Samples were preserved immediately after collection in amber-colored glass bottles containing 3–4 ml Lugol's iodine solution and several drops of concentrated formaldehyde, following the protocol of Kürten et al. (2015). Chlorophyll-*a* and inorganic nutrient concentrations were measured in the laboratory using a Shimadzu UV 1700 UV spectrophotometer, following the standard methods described by Parsons et al. (1984). Phytoplankton abundance was assessed using the Utermöhl method with an inverted microscope (Leica DMI 3000B) and Sedgewick-Rafter counting chamber. After homogenization, a 1 mL aliquot was transferred to the chamber and allowed to settle. Four randomly selected transects, each comprising 200 squares, were examined per sample. Abundance (cells m^{-3}) was calculated based on triplicate counts using the following standard formula:

Phytoplankton abundance (cells m^{-3}) = (N × Vt × 10^6) / Vc.

Where, N is the average number of cells counted per chamber (from triplicate counts and transects), Vt stands for the total volume of concentrated sample (ml), Vc is the volume of sample settled in the chamber (ml), and 10^6 is the conversion factor from mL to m^3.

Phytoplankton species were identified using standard taxonomic keys (Taylor, 1976; Tomas, 1997; Hallegraeff, 2003; Gómez, 2013). Species names were cross-verified with current nomenclature from the World Register of Marine Species (WoRMS, www.marinespecies.org) and AlgaeBase (www.algaebase.org). Harmful algal species identified in this study were categorized based on the UNESCO-IOC taxonomic reference list of harmful microalgae (https://www.marinespecies.org/hab).

Data interpretation and statistical analysis

Various statistical and visualization tools were employed for data analysis, including SPSS (version 23), PAST (version 3.1), PRIMER 6, and SURFER 8, to analyze physical, chemical, and biological parameters and to visualize spatial trends. Relationships among key physical, chemical, and biological variables were assessed using Pearson's correlation coefficients (r). Statistically significant differences in measured parameters both among stations and between depth layers were assessed using one-way analysis of variance (ANOVA). Non-metric multidimensional scaling (MDS), based on the Bray–Curtis similarity index, was applied to assess patterns in phytoplankton abundance and community composition across the sampling stations. Diversity metrics, including species richness, dominance, Pielou's evenness, and the Shannon–Wiener diversity index, were calculated using PRIMER 6 to evaluate spatial patterns in phytoplankton community structure (Clarke & Warwick, 2001). A cumulative dominance plot (k-dominance curve) was constructed to illustrate the relative dominance of species and the ecological characteristics of each station based on species rank abundance.

Results

Physical parameters

Water temperature varied significantly both spatially ($F = 3.712$, $p < 0.05$) and with depth ($F = 7.927$, $p < 0.01$, Supplementary Materials Tables S1) (Fig. 2A). Temperatures in NRS stations were higher than those in other stations in GoA. The highest surface water temperature (23.91 °C) was measured at station NRS 2, whereas the lowest (22.8 °C) at station GoA 1. During the study, the highest mean water temperature (23.25 °C ± 0.46 SD) was recorded at station NRS1 for the integrated water column, whereas the lowest water temperature (22.32 °C ± 0.39) was observed at station GoA 1 (Fig. 2A). The salinity also showed significant difference both between the stations ($F = 6.862$, $p < 0.01$, Supplementary Materials Tables S1) as well as between different depths ($F = 3.564$, $p < 0.05$). The spatial differences in salinity were more prominent than the vertical differences (Fig. 2B). Salinity was generally higher at GoA stations compared to NRS stations, with the highest value (40.65) recorded at 200 m depth at GoA 1 and the lowest salinity (40.09) in the surface waters at station NRS 2. Similarly, the highest and lowest integrated water column salinities were measured at GoA 1 (40.53 ± 0.07) and NRS 2 (40.30 ± 0.12), respectively (Fig. 2B). The observed DO values remained relatively stable during the study period, averaging 6.61 mg l^{-1} ± 0.11 (Fig. 2C).

Inorganic nutrients

Generally, nitrate and silicate contents at GoA 1 were slightly higher compared to those at other stations (Fig. 3A-E). Only ammonia showed considerable spatial variation ($F = 8.717$, $p < 0.01$, Supplementary Materials Tables S1), with negligible differences observed at different depths. All nutrients, except ammonia, showed marked vertical variation, with higher concentrations near the surface. For example, the highest concentration of nitrate (5.38 μg l^{-1}) was recorded in surface water of the GoA 1 station. However, the lowest nitrate value (0.79 μg l^{-1}) was measured in deep waters of different stations with a clear variation ($F = 10.159$, $p < 0.01$, Supplementary Materials Tables S1) (Fig. 3A). Nitrite concentrations fluctuated between 0.11 to 0.31 μg l^{-1}, with an average of 0.17 ± 0.06 μg l^{-1}. Considerable variations ($F = 17.927$, $p < 0.01$, Supplementary Materials Tables S1) were witnessed in nitrite concentrations at different depths (Fig. 3B). Similar to nitrite concentrations, ammonia concentrations were also low, with minimum and maximum concentrations being 0.08 μg l^{-1} and 0.23 μg l^{-1} (average: 0.12 ± 0.05 μg l^{-1}), respectively (Fig. 3C). On the other hand, silicate concentrations were similar to the nitrate concentrations and varied between 0.80 and 5.31 μg l^{-1}. However, the vertical distribution of silicates exhibited less variation ($F = 3.149$, $p < 0.05$, Supplementary Materials Tables S1) than both the nitrate and nitrite (Fig. 3D). Phosphate remained low and relatively uniform across stations (average: 0.06 ± 0.02μg l^{-1}), indicating phosphorus limitation in the system (Fig. 3E).

Phytoplankton biomass (chlorophyll-a)

Chlorophyll-*a* concentrations, representing phytoplankton biomass, exhibited substantial variation ($F = 15.821$, $p < 0.01$, Supplementary Materials Tables S1) at different depth layers of the water column (Fig. 3F). Chlorophyll-*a* concentrations were negligible (<0.05 mg m^{-3}) at 200 m across all stations. The DCM layer (60–70 m) consistently exhibited the highest biomass and highest chlorophyll-*a* value. DCM layer exhibited almost similar distribution for each station (Fig. 3F). GoA 1 demonstrated relatively lower phytoplankton biomass (0.15 ± 0.09 mg m^{-3}) than the other GoA stations (0.28 ± 0.15 mg m^{-3} for GoA 2 and 0.40 ± 0.22 mg m^{-3} for GoA 3). The maximum chlorophyll-*a* value (0.68 mg m^{-3}) for the GoA was observed in the DCM layer of station GoA 3, whereas the minimum (0.02 mg m^{-3}) was reported at a

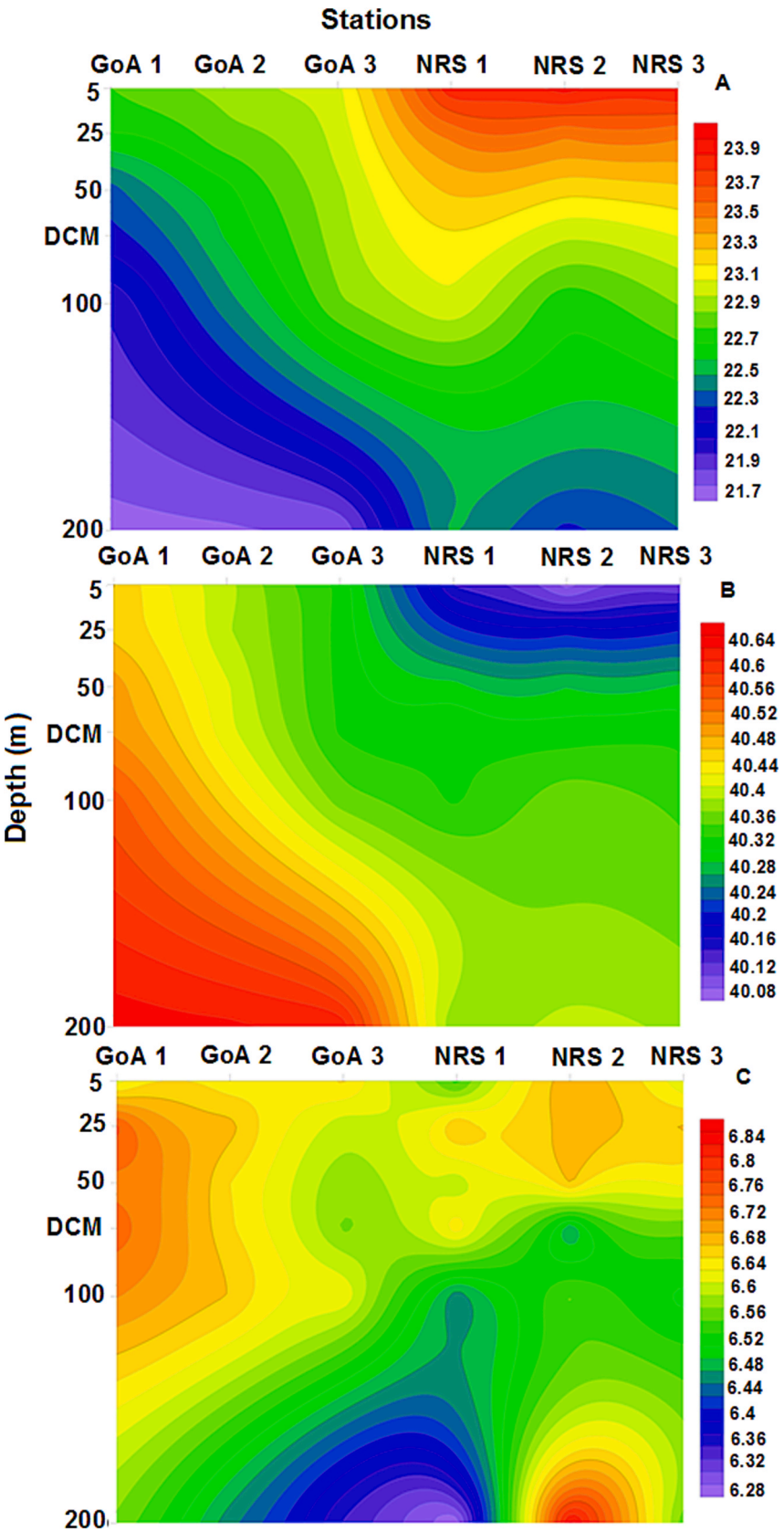

Fig. 2. Vertical profiles of water column physical parameters (A) temperature (°C), (B) salinity and (C) dissolved oxygen (mg l^{-1}) obtained during the study period.

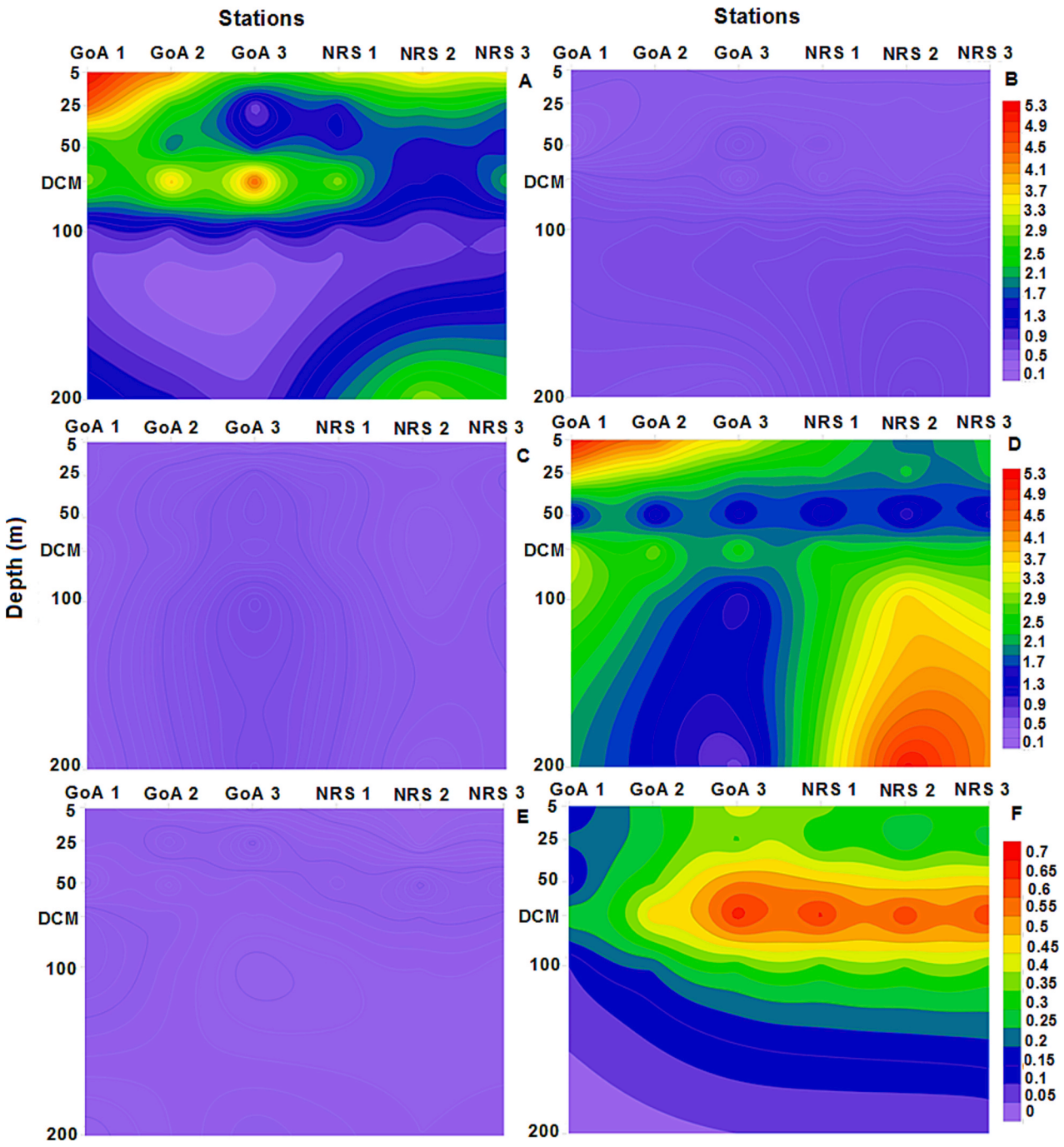

Fig. 3. Vertical profiles of inorganic nutrients (μg l^{-1}): (A) nitrate, (B) nitrite, (C) ammonia, (D) silicate, (E) phosphate and (F) chlorophyll-*a* (mg m^{-3}) at different studied stations.

depth of 200 m. All NRS stations demonstrated almost uniform chlorophyll-*a* distribution in its vertical profile. However, the maximum concentration (0.67 mg m^{-3}) was observed in the DCM of NRS 1 (Fig. 3F). Chlorophyll-*a* concentration oscillated between 0.05 and 0.67 mg m^{-3}. Nevertheless, its concentration at 200 m in NRS 1 were similar to GoA stations.

Phytoplankton abundance and spatial distribution

Phytoplankton abundance fluctuated between 26 × 10^3 cells m^{-3} (GoA 1) and 51.9 × 10^3 cells m^{-3} (GoA 3) with an average of 40.2 ± 9 × 10^3 cells m^{-3}. In GoA, the total density followed a decreasing pattern from south to north, whereas inter-station density variations in the NRS region were lower (35.4–45.7 × 10^3 cells m^{-3}) (Fig. 4A). Diatoms contributed considerably (46–72 %) towards the total phytoplankton density (Fig. 4B). The abundance of diatoms fluctuated between 13.2 × 10^3 cells m^{-3} (GoA 1) and 37.4 × 10^3 cells m^{-3} (average: 22.6 ± 7.8 × 10^3 cells m^{-3}) (GoA 3). Autotrophic dinoflagellates were the dominant phytoplankton at station GoA 1 (48 %) and marginally so at stations NRS 2 (43 %) and NRS 3 (41 %) (Fig. 4B). Dinoflagellate density ranged between 11 × 10^3 cells m^{-3} and 19.9 × 10^3 cells m^{-3} at NRS 1 and NRS 2, respectively (Fig. 4A). The cyanophytes contributed a minor fraction (from 1 to 10 %) towards the total phytoplankton density, and the density fluctuated between 1 × 10^3 cells m^{-3} and 10 × 10^3 cells m^{-3} (Fig. 4A).

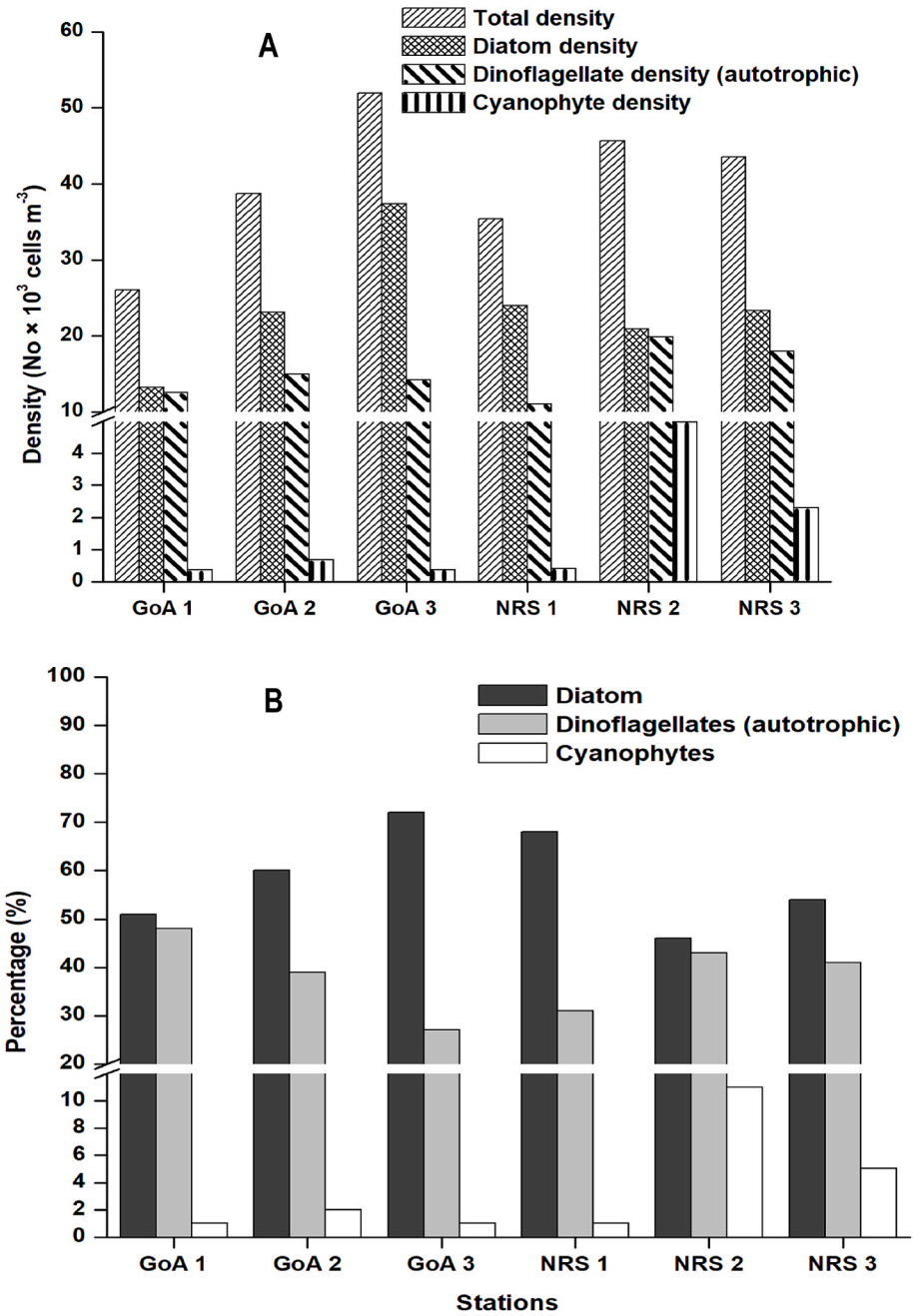

Fig. 4. Density (A) and percentage (B) of heterotrophic dinoflagellates, ciliates and dinoflagellate cysts in the study period.

Heterotrophic dinoflagellates, ciliates and dinoflagellate cysts

The abundance of heterotrophic dinoflagellates, ciliates, and dinoflagellate cysts exhibited spatial variability between the GoA and the NRS stations (Fig. 5). Among the GoA stations, heterotrophic dinoflagellate densities ranged from 4.11 to 4.76 $\times$ 10^3 cells m^{-3}, with the highest value recorded at GoA 2 (4.76 $\times$ 10^3 cells m^{-3}) and the lowest at GoA 3 (4.11 $\times$ 10^3 cells m^{-3}) (Fig. 5). Ciliate concentrations varied across GoA, with concentrations being 2.29 $\times$ 10^3 cells m^{-3} at GoA 2 and 3.57 $\times$ 10^3 cells m^{-3} at GoA 1. Dinoflagellate cyst abundance was highest at GoA 1 (5.35 $\times$ 10^3 cells m^{-3}) and lowest at GoA 3 (1.87 $\times$ 10^3 cells m^{-3}) (Fig. 5). In contrast, the NRS stations displayed a broader range in organism densities. Heterotrophic dinoflagellate abundance peaked at NRS 3 with 6.88 $\times$ 10^3 cells m^{-3}, whereas the lowest was observed at NRS 2 (4.31 $\times$ 10^3 cells m^{-3}) (Fig. 5). Ciliate densities exhibited a pronounced peak at NRS 2 (8.28 $\times$ 10^3 cells m^{-3}), which substantially exceeded values at NRS 1 and NRS 3 (4.08 and 3.57 $\times$ 10^3 cells m^{-3}, respectively). Dinoflagellate cysts also reached their maximum at NRS 2 (9.94 $\times$ 10^3 cells m^{-3}) (Fig. 5).

Phytoplankton community composition and species diversity

In total, 179 phytoplankton species were identified in the present study (Supplementary Materials Tables S2). Dinoflagellates dominated the species composition with 100 species, out of which 27 were the heterotrophic ones, whereas diatoms were represented by 78 species, with centric forms (51 species) being more prevalent than pennate forms (27 species). Cyanophytes were symbolized by only a single species. Higher number of species (S) were reported from station NRS 2 (104), followed by NRS 3 (103) and GoA 2 (100), whereas the number of species at other three stations was low, ranging between 80 and 82 (Fig. 6A). Species dominance (D) was considerably higher in station GoA

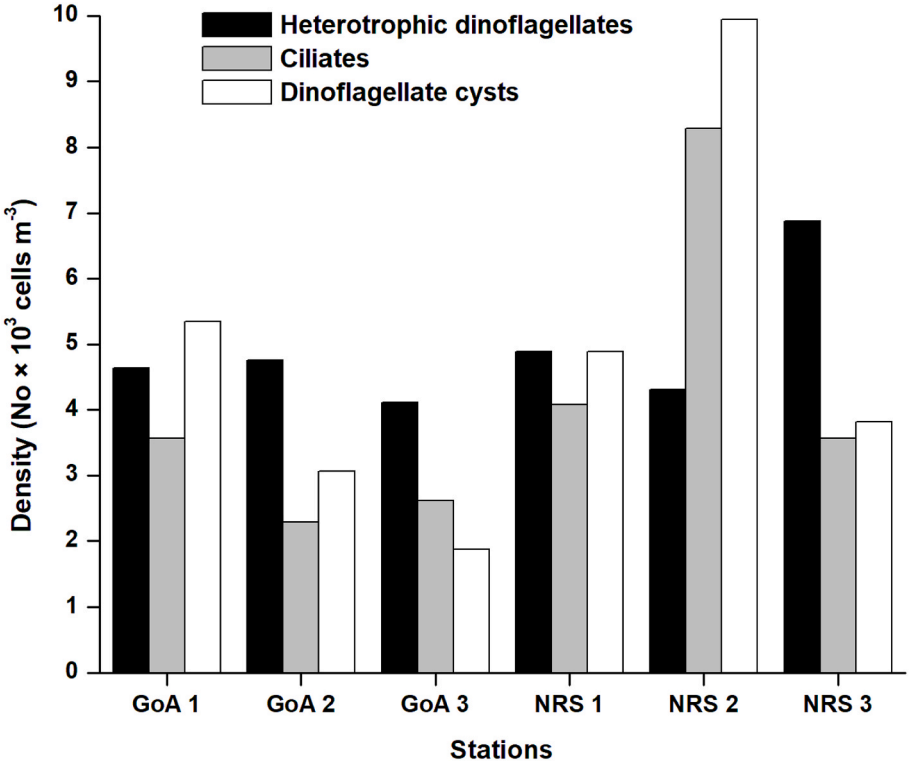

Fig. 5. Density of heterotrophic dinoflagellates, ciliates and dinoflagellate cysts during the study period.

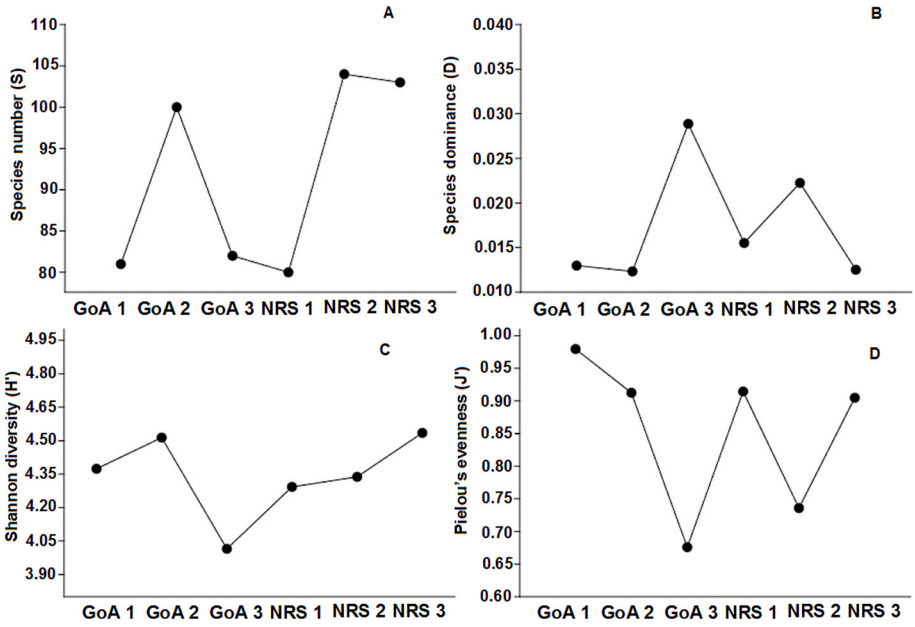

Fig. 6. Various biodiversity indices on the microphytoplankton species composition during the study period.

3, followed by station NRS 2 (Fig. 6B). The Shannon diversity index (H') values fluctuated between 3.95 (GoA 3) and 4.50 (GoA 2 and NRS 3), whereas the Pielou's evenness index (J') displayed its higher values in GoA 1 and lower in GoA 3 (Fig. 6C-D).

The MDS plot, derived from Bray–Curtis similarity of phytoplankton species composition, indicated a 50 % similarity across all stations except between stations GoA 2 and NRS 3, which exhibited a 60 % similarity (Fig. 7A). The cumulative dominance plot showed that GoA 3 had the most even species distribution, whereas NRS 2 was dominated by fewer species, indicating lower evenness (Fig. 7B). Genus *Chaetoceros* comprised a maximum species number (19 species) in diatoms followed by the genera of *Guinardia, Rhizosolenia, Pleurosigma* and *Pseudo-nitzschia* (4 species each). Dinoflagellates witnessed the diversity of genus *Tripos* with a total of 30 different species, which is closely followed by genus *Protoperidinium* (22 species). Three of the dinoflagellate species reported in the present study—*Podolampas elegans* Schütt, 1895; *Pronoctiluca acuta* (Lohmann) Schiller, 193; and *P. pelagica* Fabre-Domergue, 1889—were documented as new records for the Red Sea. Three diatom species and seven dinoflagellate species that cause severe algal bloom worldwide were also recorded during the current research

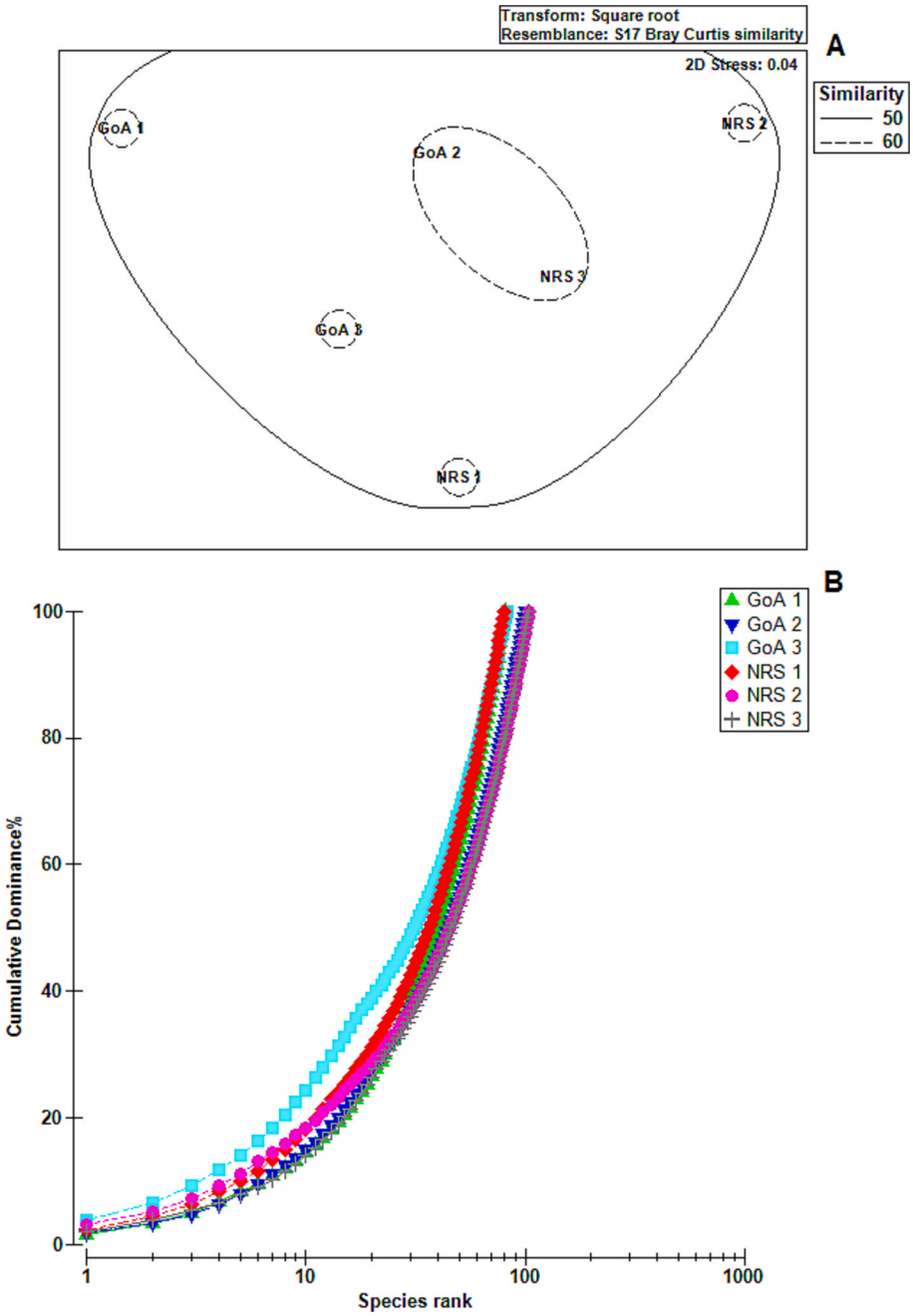

Fig. 7. MDS (A) derived from the Bray-Curtis similarity index of the species diversity and cumulative dominance plot (B) based on species rank obtained for the species community composition during the study period.

(Supplementary Materials Tables S2). The diatom species included *Pseudo-nitzschia cuspidata* (Hasle) Hasle, 1993; *Pseudo-nitzschia delicatissima* (Cleve) Heiden, 1928; and *Pseudo-nitzschia seriata* (Cleve) H. Peragallo, 1899. The seven dinoflagellates species included *Gonyaulax spinifera* (Claparède & Lachmann) Diesing, 1866; *Lingulaulax polyedra* (F. Stein) M. J. Head, K. N. Mertens & R. A. Fensome, 2024; *Phalacroma mitra* F. Schütt, 1895; *Phalacroma rotundatum* (Claparéde & Lachmann) Kofoid & Michener, 1911; *Prorocentrum cordatum* (Ostenfeld) J.D. Dodge, 1975; *Prorocentrum lima* (Ehrenberg) F.Stein, 1878; and *Prorocentrum mexicanum* Osorio-Tafall, 1942 (Ehrenberg) F. Stein, 1878. Cyanophytes were represented by only one genus (*Trichodesmium* sp.), which is regarded as a common inhabitant of the Red Sea waters.

Statistical analyses

Statistical analysis revealed several significant patterns in the environmental variables across stations and depths. One-way ANOVA showed that temperature, salinity, chlorophyll-*a*, nitrate (NO_3^-), nitrite (NO_2^-), ammonia (NH_4^+), and silicate (SiO_4^{4-}) exhibited significant variations across stations or at different depths ($p < 0.05$, Supplementary Materials Tables S1). Notably, temperature and salinity varied significantly across both stations and depths, indicating spatial and vertical gradients. Chlorophyll-*a*, nitrate, nitrite, and silicate concentrations were significantly affected by depth, whereas ammonia showed significant differences between stations (Supplementary Materials Tables S1). Pearson correlation analysis further highlighted key associations between phytoplankton-related variables and environmental factors (Supplementary Materials Tables S3). Chlorophyll-*a* concentration

exhibited a positive correlation with temperature ($r = 0.569$, $p < 0.01$) and a negative correlation with salinity ($r = -0.510$, $p < 0.01$). Additionally, chlorophyll-*a* was negatively correlated with nitrite ($r = -0.375$, $p < 0.05$). Among nutrients, nitrate (NO_3^-) was positively correlated with dissolved oxygen ($r = 0.346$, $p < 0.05$) and silicate ($r = 0.520$, $p < 0.01$), while nitrite (NO_2^-) was negatively correlated with temperature ($r = -0.484$, $p < 0.01$) and nitrate ($r = -0.444$, $p < 0.01$). Ammonia (NH_4^+) was negatively associated with dissolved oxygen ($r = -0.414$, $p < 0.05$) and silicate ($r = -0.483$, $p < 0.01$).

Discussion

Nutrient scarcity represents one of the primary constraints on primary productivity in NRS and GoA regions (Al-Qutob et al., 2002; Labiosa et al., 2003). Our results confirmed the findings of the previous reports (Stambler, 2006; Labiosa et al., 2003) that early spring in GoA is marked by strong convective mixing, extending to 400–600 m, which enriches the euphotic zone. Despite the geographic proximity, GoA and NRS exhibited contrasting physical regimes, which is consistent with observations of Badran (2001) and Genin et al. (1995). This phenomenon was particularly distinct during the present study, which is similar to the findings of Stambler (2005, 2006). Within GoA, both the temperature and salinity variations displayed a gradient, with temperature tending to decrease and salinity tending to increase towards north (Stambler, 2005).

The physical characteristics of GoA and NRS observed in the present study aligned closely with results from earlier research conducted in the spring (Grossart & Simon, 2002; Stambler, 2006; Iluz et al., 2009; Dishon et al., 2012; Carlson et al., 2014; Kheireddine et al., 2017; Pearman et al., 2017). It is well documented that during winter and early spring, deep convection in the GoA is sufficiently strong to mix the water column down to depths of 400–600 m (Labiosa et al., 2003; Stambler, 2006); this phenomenon was clearly reflected in the findings of the present research. Minimal differences were observed in the distribution of physical parameters of the NRS compared to that of GoA, indicating the presence of a uniform water mass in NRS during the spring season (Stambler, 2005). The higher concentration of dissolved oxygen obtained throughout the water column was mainly due to the stability between the interplay of oxygen utilization and reproduction in the euphotic zone alongside mixing of deeper waters (Badran, 2001). The present study revealed a significant positive correlation between temperature and chlorophyll-*a,* which suggests that phytoplankton proliferation in both GoA and NRS depend on temperature and convective mixing (Kimor & Golandsky, 1977; Labiosa et al., 2003; Triantafyllou et al., 2014). Salinity, in turn, displayed a negative correlation with chlorophyll-*a* content largely due to the lower phytoplankton biomasses in the northern parts of GoA.

The present study was conducted during a period of active mixing, which brings adequate nutrient source to the surface photic layer (Labiosa et al., 2003; Post et al., 2011). However, the observed inorganic nutrient levels still indicated the oligotrophic nature of the region. Despite ongoing convective mixing, nutrient concentrations remained low, possibly due to active phytoplankton uptake during the bloom phase, leading to rapid depletion of surface nutrients (Al-Najjar et al., 2007; Dishon et al., 2012). The nutrient concentrations observed in the present study were comparable to those described by Klinker et al. (1978) and Fuller et al., (2005). However, they were relatively lower than those documented in other studies conducted in both GoA and NRS during spring (Lindell & Post, 1995; Al-Qutob et al., 2002; Stambler, 2005; Al-Najjar et al., 2007; Wafar et al., 2016). The minimal vertical variation of ammonia in the present study are may be attributed to the rapid nitrification and photosynthetic consumption, which results in the sequestration of the particular nutrients in the euphotic layer (Badran, 2001). The occurrence of various nutrients in the water column of GoA is attributed to different processes, such as thermal stratification-destratification and primary productivity (Badran, 2001). Although slightly higher nutrient concentrations were observed at GoA 1, phytoplankton biomass remained lower compared to those at GoA 2, GoA 3, and the NRS stations. In the northern GoA, the existence of two anticyclonic and one cyclonic eddies during winter and spring, respectively, might have increased the nutrient levels (Al-Najjar et al., 2007). The phytoplankton increase occurred much later in the northern gulf than the other parts, which is solely responsible for the occurrence of lower biomass in this region (Labiosa et al., 2003). The NRS stations observed with minimal spatial as well as vertical differences in the nutrient distribution clearly depict the presence of a uniform water mass during early spring (Stambler, 2005). The different inorganic nutrients measured during the study exhibited weak statistical correlations with phytoplankton biomass, which may partly be attributed to the limited number of data points per sector ($n = 15$), which likely reduced the statistical power to detect significant relationships. Similarly, Al-Najjar et al. (2007) reported that statistical correlation is poor likely because of temporal lag between the nutrient increase welded from vertical mixing and the response of phytoplankton towards this enhancement.

In the present study, chlorophyll $-a$ concentrations representing phytoplankton biomass clearly displayed the occurrence of vertical mixing in the study region. Additionally, the phytoplankton values reported in the present study were in agreement with the result of previous studies conducted in GoA (e.g. Lindell & Post, 1995; Badran, 2001; Grossart & Simon, 2002; Stambler, 2006; Iluz et al., 2009) as well as in NRS (Berninger & Wickham, 2005; Stambler, 2005; Dishon et al., 2012; Racault et al., 2015; Kheireddine et al., 2017; Pearman et al., 2017). Early spring chlorophyll-*a* concentrations in the present study were considerably higher than those obtained for other seasons in both the NRS and GoA (Labiosa et al., 2003; Acker et al., 2008; Qurban et al., 2014; Devassy et al., 2017). In the present study, chlorophyll-*a* peak was observed at depths of 60–70 m in the water column, indicating the occurrence of a possible DCM, which is consistent with stratified conditions, where optimal light availability intersects with nutrient enrichment from mixing layers (Stambler, 2005, 2006; Qurban et al., 2014; Kheireddine et al., 2017; Pearman et al., 2017). In the present study, DCM was consistently observed at depths between 60–70 m across all stations, which aligns well with the previous findings in the region. For instance, Stambler (2005) and Qurban et al. (2014) reported DCM depths ranging from 60 to 90 m in the GoA and NRS during spring. Similarly, Iluz et al. (2009) found the DCM typically occurred at 60–75 m during short-term diatom blooms in the GoA. These comparisons support the consistency of DCM positioning in the water column during spring mixing, which is likely influenced by light penetration and nutrient availability. The uniformity of the water column in the NRS was further reflected in the distribution of phytoplankton biomass, which showed a consistent pattern throughout this region. In GoA, however, a clear gradient was detected, where chlorophyll-*a* concentrations tended to decrease toward the northern region of GoA. The southernmost station in GoA (GoA 3), which is located near to the Strait of Tiran exhibited higher chlorophyll values. It was mainly due to the wind regime in the GoA during the spring, which is more intense towards the southern end. Such intense winds can create upwelling and Ekman drift, which in turn increases the phytoplankton productivity in the region (Berman et al., 2000; Labiosa et al., 2003). Elevated chlorophyll concentrations at GoA 3 likely result from wind-driven upwelling and tidal mixing near the Strait of Tiran, which enhances nutrient flux into surface waters (Murray et al., 1984; Labiosa et al., 2003).

In both GoA and NRS, primary productivity is predominantly driven by ultraphytoplankton, particularly those smaller than 8 μm in size, while the contribution of microphytoplankton remains minimal (Lindell & Post, 1995; Sommer, 2000). The present study recorded a significantly greater density of microphytoplankton (> 20 μm) in the spring season, suggesting that spring offers more favorable conditions for their growth than the summer season (Devassy et al., 2017; El-Sherbiny et al., 2019). Hence, microphytoplankton density varies seasonally, with spring possibly supporting higher abundances within the studied area.

However, given the limited spatial and temporal scope of sampling, further investigation is needed to confirm whether this pattern is consistent across broader scales in these predominantly ultraphytoplankton-dominated waters. Furthermore, due to the uniform water mass, the distribution pattern of phytoplankton abundance and composition in the NRS region was more uniform compared to that in GoA, where the phytoplankton density exhibited a decreasing trend from south to north. Stratification begins much earlier in NRS than GoA, which results in the formation of a stable water column and uniform water mass throughout the region (Stambler, 2005). This may have resulted in the minimal differences obtained in the phytoplankton density from the NRS stations. The highest phytoplankton density during the study was recorded in the station located near the Strait of Tiran (GoA 3). Within GoA, GoA 3 was the most productive station owing to the continuous water exchange between NRS and GoA, presence of strong winds that create slight upwelling, and shallower waters makes this station (Genin et al., 1995; Plähn et al., 2002). While studying the microbial food web in GoA and NRS regions, Berninger and Wickham (2005), reported higher microphytoplankton densities from the Strait of Tiran. The present study revealed a surge in microphytoplankton densities in GoA region during the mixing period (Klinker et al., 1978; Stambler, 2006; Dishon et al., 2012). Multiple variables, such as temperature, nutrient concentrations, and water column stability and grazing, determine the succession of different phytoplankton groups in the highly oligotrophic regions, such as GoA and NRS (Lindell & Post, 1995). During summer, minimal availability of nutrients results in the region being dominated by ultraphytoplankton. In contrast, the concentration of microphytoplankton such as diatoms and dinoflagellates proliferate is high during spring, during which the distribution of nutrients in the water column increases (Kimor & Golandsky, 1977; Stambler, 2006). Diatoms formed the dominant group at stations GoA 2, GoA 3, and NRS 1 during the early spring, whereas dinoflagellates partially dominated in the other stations (GoA 1, NRS 2 and NRS 3), along with diatoms. A similar pattern of diatom dominance in the GoA during the early spring (March) has been reported previously (Post et al., 2002; Al-Najjar et al., 2007). However, several studies have reported the dominance of dome filamentous cyaophycean during summer (Post et al., 2002; Al-Najjar et al., 2007; Devassy et al., 2017). In the present study, the cyanophytes were represented by only the native *Trichodesmium* sp. that showed low densities in both regions during the study. The current study also observed the presence of heterotrophic dinoflagellates, ciliates (microzooplankton) and many dinoflagellate cysts within the study region, implying the possible existence of a 'microbial loop during the spring period. Sommer et al. (2002) demonstrated that microzooplankton grazing on phytoplankton in both NRS and GoA is predominant during spring, with grazing intensity increasing in summer when ultraphytoplankton dominate the community (Pearman et al., 2017). Additionally, Kimor and Golandsky-Baras (1981) reported the dominance of microzooplankton—particularly tintinnids—alongside diatoms and dinoflagellates during March. Dinoflagellates were the dominant group among the phytoplankton species, indicating their high diversity within the GoA and NRS regions. The dominance of dinoflagellates within the microphytoplankton diversity of the Red Sea has been reported by many studies (Ismael, 2015; Prabowo & Agusti, 2019; Al-Amri et al., 2020; El-Sherbiny et al., 2021). Devassy et al. (2017) investigated the spatial variation of phytoplankton from NRS during summer and reported the prevailing presence of dinoflagellates in the phytoplankton community. Furthermore, its dominance in GoA has been previously mentioned by Al-Najjar et al. (2007) and El-Sherbiny et al. (2019). The findings of the present study, which was carried out during early spring, revealed that the dinoflagellates dominate the microphytoplankton community composition of GoA and NRS irrespective of the season. Within the diatoms, centric species were particularly dominant, with a higher number of species belonging to the genus *Chaetoceros*, which has been reported previously (Post et al., 2002; Al-Najjar et al., 2007; Iluz et al., 2009). The dinoflagellate community was dominated by two genera of order Gonyaulacales (autotrophic dinoflagellate *Tripos* and heterotrophic dinoflagellate *Protoperidinium*). The predominance of *Chaetoceros* (a bloom-forming diatom genus) and dinoflagellate genera *Tripos* and *Protoperidinium* reflects their adaptive including, fast growth, cyst formation, and vertical migration capabilities, in oligotrophic, seasonally mixed environments (Post et al., 2002; Ismael, 2015; Devassy et al., 2017). The diversity indices revealed spatial variability in phytoplankton community structure across the study area. The highest species richness was observed at NRS 2 and NRS 3, suggesting more taxonomically diverse communities in these stations. Shannon–Wiener diversity index (H') values ranged from 3.95 to 4.50, with the highest values at GoA 2 and NRS 3, indicating relatively high diversity and balanced species distribution at these stations. In contrast, GoA 3 exhibited lower diversity (H' = 3.95) and higher dominance (D), suggesting that the community was more heavily influenced by a few dominant species. This pattern was further supported by the low evenness (J') at GoA 3, indicating that species were not uniformly distributed. Hence, phytoplankton communities in the southern part of GoA may be more ecologically structured or subjected to selective environmental pressures compared to the more uniform communities in the NRS. Table 1 presents a comparison of microphytoplankton biomass, species richness, and abundance observed in the present study and those reported previously in GoA and NRS. The phytoplankton biomass and abundance observed in the present study of GoA and NRS during spring are generally in agreement with previous investigations conducted in the region, primarily during summer (Devassy et al., 2017; El-Sherbiny et al., 2019). However, phytoplankton biomass (as chlorophyll-*a*) was slightly lower than the values reported in earlier studies conducted during the winter period (Lindell & Post, 1995; Stambler, 2006). Significantly higher phytoplankton abundances have also been documented in studies from the coastal waters of both GoA and NRS. For instance, Madkour et al. (2010) and Nassar (2007) in GoA, and Nassar et al. (2014) in the Egyptian NRS, reported higher phytoplankton densities and lower number of species in coastal water, which was likely driven by increased nutrient inputs, shallower water columns, and enhanced vertical mixing or upwelling. These findings highlight the strong spatial variability in phytoplankton dynamics across the Red Sea and emphasize the influence of hydrographic setting-particularly the distinction between offshore and coastal zones-on community structure and productivity.

Conclusion

Our findings highlighted the distinct microphytoplankton dynamics during the spring period in GoA and NRS. Physical, chemical, and biological parameters exhibited a south-to-north gradient in GoA. In contrast, the NRS behaved as a relatively uniform water mass. Phytoplankton biomass and cell density were lower in the northernmost GoA station, whereas NRS stations showed minimal spatial variations. DCM, observed consistently between 60 and 70 m across all stations, marked the peak in phytoplankton biomass. The dominant microphytoplankton groups included diatoms and dinoflagellates, with dinoflagellates exhibiting higher species richness (100 taxa of which 27 were heterotrophic) compared to diatoms (78 taxa), and cyanophytes playing a negligible role. Although many heterotrophic dinoflagellates ciliates, and dinoflagellate cysts were recorded, no clear evidence of active trophic interactions or bloom events was found. The findings suggest that microphytoplankton distribution in both regions is shaped by water column structure, nutrient variability, and regional hydrographic patterns during the spring season.

CRediT authorship contribution statement

Mohsen M. El-Sherbiny: Writing – review & editing, Writing – original draft, Visualization, Funding acquisition, Formal analysis, Data curation, Conceptualization. **Zaki M. Al-Hasawi:** Writing – original

Table 1
Comparative summary of chlorophyll-*a* concentrations (mg m^{-3}), phytoplankton species number, and abundance (cells m^{-3}; averages in brackets) from the current study and previous studies conducted in the Gulf of Aqaba and the Northern Red Sea.

Region	Season	Chlorophyll-*a*	Species Number	Phytoplankton Abundance	References
GoA & NRS	Spring	0.02 – 0.68	179	30.7– 56.1 × 10^3 (45.2 × 10^3)	Current Study
GoA	Summer	0.17–0.27	138	24.2—41.5 × 10^3 (32.44 × 10^3)	El-Sherbiny et al., 2019
GoA	Spring	–	82	(21374 × 10^3)	Nassar, 2007
GoA	Winter–Spring	0.5 – 1.0	–	–	Lindell & Post, 1995
NRS (Al Khoraeyba area)	Summer	0.04–0.13	97	10–85 × 10^3 (44 × 10^3)	Devassy et al., 2017
NRS	Spring	0.143	> 40	(2000 × 10^3)	Madkour et al., 2010
NRS	Winter	0.6 – 1.2	–	–	Stambler, 2006
Egyptian coastal waters of NRS	Spring	–	145	(5282 × 10^3)	Nassar et al., 2014

draft, Validation, Resources, Data curation, Conceptualization. **Mohamed E. EL-Hefnawy:** Writing – original draft, Visualization, Software, Resources, Funding acquisition.

Declaration of competing interest

The authors declare that they have no known competing financial interests or personal relationships that could have appeared to influence the work reported in this paper.

Acknowledgements

This project was funded by the Deanship of Scientific Research (DSR) at King Abdulaziz University, Jeddah, Saudi Arabia, under the grant no. (IPP: 108-150-2025). The authors, therefore, acknowledge with thanks DSR for technical and financial support. We further extend our gratitude towards the captain and the crew members of *RV Thuwal* for the support provided in order to complete the sampling programs on time.

Appendix A. Supplementary data

Supplementary data to this article can be found online at https://doi.org/10.1016/j.ejar.2025.09.001.

References

Acker, J., Leptoukh, G., Shen, S., Zhu, T., & Kempler, S. (2008). Remotely-sensed chlorophyll *a* observations of the northern Red Sea indicate seasonal variability and influence of coastal reefs. *Journal of Marine Systems, 69*(3–4), 191–204. https://doi.org/10.1016/j.jmarsys.2005.12.006

Al-Amri, A. A., Qari, H. A., & El-Sherbiny, M. M. (2020). Distribution and community structure of microphytoplankton in relation to increasing anthropogenic impact along coastal waters of Jeddah, the central Red Sea. *Oceanological and Hydrobiological Studies, 49*(2), 193–205. https://doi.org/10.1515/ohs-2020-0018

Al-Najjar, T., Badran, M. I., Richter, C., Meyerhoefer, M., & Sommer, U. (2007). Seasonal dynamics of phytoplankton in the Gulf of Aqaba, Red Sea. *Hydrobiologia, 579*, 69–83. https://doi.org/10.1007/s10750-006-0365-z

Al-Qutob, M., Häse, C., Tilzer, M. M., & Lazar, B. (2002). Phytoplankton drives nitrite dynamics in the Gulf of Aqaba, Red Sea. *Marine Ecology Progress Series, 239*, 233–239. https://doi.org/10.3354/meps239233

Badran, M. I. (2001). Dissolved oxygen, chlorophyll *a* and nutrients: Seasonal cycles in waters of the Gulf of Aqaba, Red Sea. *Aquatic Ecosystem Health & Management, 4*(2), 139–150. https://doi.org/10.1080/14634980127711

Berman, H., & Gildor, H. (2022). Phytoplankton bloom in the Gulf of Elat/Aqaba: Physical versus ecological forcing. *Journal of Geophysical Research: Oceans, 127*(5), Article e2021JC017922.

Berman, T., Paldor, N., & Brenner, S. (2000). Simulation of wind-driven circulation in the Gulf of Elat (Aqaba). *Journal of Marine Systems, 26*(3–4), 349–365. https://doi.org/10.1016/S0924-7963(00)00045-2

Berninger, U. G., & Wickham, S. A. (2005). Response of the microbial food web to manipulation of nutrients and grazers in the oligotrophic Gulf of Aqaba and northern Red Sea. *Marine Biology, 147*, 1017–1032. https://doi.org/10.1007/s00227-005-1565-1

Carlson, D. F., Fredj, E., & Gildor, H. (2014). The annual cycle of vertical mixing and restratification in the Northern Gulf of Eilat/Aqaba (Red Sea) based on high temporal and vertical resolution observations. *Deep Sea Research Part i: Oceanographic Research Papers, 84*, 1–17. https://doi.org/10.1016/j.dsr.2013.10.004

Clarke, K. R., & Warwick, R. M. (2001). Change in marine communities. *An Approach to Statistical Analysis and Interpretation, 2*, 1–168.

Devassy, R. P., El-Sherbiny, M. M., Al-Sofyani, A. M., & Al-Aidaroos, A. M. (2017). Spatial variation in the phytoplankton standing stock and diversity in relation to the prevailing environmental conditions along the Saudi Arabian coast of the northern Red Sea. *Marine Biodiversity, 47*, 995–1008. https://doi.org/10.1007/s12526-017-0693-4

Dishon, G., Dubinsky, Z., Caras, T., Rahav, E., Bar-Zeev, E., Tzubery, Y., & Iluz, D. (2012). Optical habitats of ultraphytoplankton groups in the Gulf of Eilat (Aqaba), Northern Red Sea. *International Journal of Remote Sensing, 33*(9), 2683–2705. https://doi.org/10.1080/01431161.2011.619209

Dreano, D., Raitsos, D. E., Gittings, J., Krokos, G., & Hoteit, I. (2016). The Gulf of Aden intermediate water intrusion regulates the southern Red Sea summer phytoplankton blooms. *PLoS One1, 11*(12), Article e0168440. https://doi.org/10.1371/journal.pone.0168440

El-Sherbiny, M. M., Al-Harbi, M. A., & Kumar, A. J. (2021). Spatio-temporal variation of microphytoplankton communities in Obhur Creek, the central Red Sea. *Oceanological and Hydrobiological Studies, 50*(1), 98–114. https://doi.org/10.2478/oandhs-2021-0010

El-Sherbiny, M. M., Devassy, R. P., Muller, E. M., Al-Sofyani, A. A., & Al-Aidaroos, A. M. (2019). Biodiversity and abundance of plankton communities along the coastal waters of Gulf of Aqaba, Saudi Arabia. *Pakistan Journal of Zoology, 51*(5), 1823. https://doi.org/10.17582/journal.pjz/2019.51.5.1823.1836

Genin, A., Lazar, B., & Brenner, S. (1995). Vertical mixing and coral death in the Red Sea following the eruption of Mount Pinatubo. *Nature, 377*(6549), 507–510. https://doi.org/10.1038/377507a0

Gómez, F. (2013). Reinstatement of the dinoflagellate genus Tripos to replace Neoceratium, marine species of *Ceratium* (Dinophyceae, Alveolata). *Cicimar Oceánides, 28*(1), 1–22. https://doi.org/10.37543/oceanides.v28i1.119

Grossart, H. P., & Simon, M. (2002). Bacterioplankton dynamics in the Gulf of Aqaba and the northern Red Sea in early spring. *Marine Ecology Progress Series, 239*, 263–276.

Hallegraeff, G. M. (2003). Harmful algal blooms: A global overview. *Manual on Harmful Marine Microalgae, 33*, 1–22.

Iluz, D., Dishon, G., Capuzzo, E., Meeder, E., Astoreca, R., Montecino, V., & Marra, J. (2009). Short-term variability in primary productivity during a wind-driven diatom bloom in the Gulf of Eilat (Aqaba). *Aquatic Microbial Ecology, 56*(2–3), 205–215. https://doi.org/10.3354/ame01321

Ismael, A. A. (2015). Phytoplankton of the Red Sea. *The Red Sea: the Formation, Morphology, Oceanography and Environment of a Young Ocean Basin, 567–583*. https://doi.org/10.1007/978-3-662-45201-1_32

Kheireddine, M., Ouhssain, M., Claustre, H., Uitz, J., Gentili, B., & Jones, B. H. (2017). Assessing pigment-based phytoplankton community distributions in the Red Sea. *Frontiers in Marine Science, 4*, 132. https://doi.org/10.3389/fmars.2017.00132

Kimor, B., & Golandsky, B. (1977). Microplankton of the Gulf of Elat: Aspects of seasonal and bathymetric distribution. *Marine Biology, 42*, 55–67.

Kimor, B., & Golandsky-Baras, B. (1981). Distribution and ecology of the tintinnids in the Gulf of Elat (Aqaba), Red Sea. *Journal of Plankton Research, 3*(3), 445–459.

Klinker, J., Reiss, Z., Kropach, C., Levanon, I., Harpaz, H., & Shapiro, Y. (1978). Nutrients and biomass distribution in the Gulf of Aqaba (Elat), Red Sea. *Marine Biology, 45*, 53–64.

Kürten, B., Khomayis, H. S., Devassy, R., Audritz, S., Sommer, U., Struck, U., & Al-Aidaroos, A. M. (2015). Ecohydrographic constraints on biodiversity and distribution of phytoplankton and zooplankton in coral reefs of the Red Sea. *Saudi Arabia. Marine Ecology, 36*(4), 1195–1214. https://doi.org/10.1111/maec.12224

Kürten, B., Zarokanellos, N. D., Devassy, R. P., El-Sherbiny, M. M., Struck, U., Capone, D. G., & Jones, B. H. (2019). Seasonal modulation of mesoscale processes alters nutrient availability and plankton communities in the Red Sea. *Progress in Oceanography, 173*, 238–255. https://doi.org/10.1016/j.pocean.2019.02.007

Labiosa, R. G., Arrigo, K. R., Genin, A., Monismith, S. G., & van Dijken, G. (2003). The interplay between upwelling and deep convective mixing in determining the seasonal phytoplankton dynamics in the Gulf of Aqaba: Evidence from SeaWiFS and MODIS. *Limnology and Oceanography, 48*(6), 2355–2368. https://doi.org/10.4319/lo.2003.48.6.2355

Laiolo, L., Barausse, A., Dubinsky, Z., Palmeri, L., Goffredo, S., Kamenir, Y., & Iluz, D. (2014). Phytoplankton dynamics in the Gulf of Aqaba (Eilat, Red Sea): A simulation study of mariculture effects. *Marine Pollution Bulletin, 86*(1–2), 481–493.

Lindell, D., & Post, A. F. (1995). Ultraphytoplankton succession is triggered by deep winter mixing in the Gulf of Aqaba (Eilat), Red Sea. *Limnology and Oceanography, 40*(6), 1130–1141.

Madkour, F., El-Sherbiny, M., & Aamer, M. (2010). Phytoplankton population along certain Egyptian coastal regions of the Red Sea. *Egyptian Journal of Aquatic Biology and Fisheries, 14*(2), 95–109.

Manasrah, R., Badran, M., Lass, H. U., & Fennel, W. (2004). Circulation and winter deep-water formation in the northern Red Sea. *Oceanologia, 46*(1).

Morcos, S. A. (1970). Physical and chemical oceanography of the Red Sea. *Oceanography and Marine Biology: An Annual Review, 8*(73), 202.

Murray, S. P., Hecht, A., & Babcock, A. (1984). On the mean flow in the Tiran Strait in winter. *Journal of Marine Research, 42*(2), 265–287.

Nassar, M. Z. (2007). Nutrients and phytoplankton distribution in the coastal waters of Aqaba Gulf, Red Sea, Egypt. *Egyptian Journal of Aquatic Research, 33*(2), 133–151.

Nassar, M. Z. A., & Fahmy, M. A. (2023). Seasonal variability of phytoplankton along some of the Red Sea harbors during 2019–2021. *Egyptian Journal of Aquatic Biology and Fisheries, 27*(2), 43–60.

Nassar, M. Z., Mohamed, H. R., Khiray, H. M., & Rashedy, S. H. (2014). Seasonal fluctuations of phytoplankton community and physico-chemical parameters of the north western part of the Red Sea, Egypt. *Egyptian Journal of Aquatic Research, 40*(4), 395–403.

Parsons, T. R., Maita, Y., & Lalli, C. M. (1984). *A manual of chemical and biological methods for seawater analysis*. Oxford: Pergamon Press.

Pearman, J. K., Ellis, J., Irigoien, X., Sarma, Y. V. B., Jones, B. H., & Carvalho, S. (2017). Microbial planktonic communities in the Red Sea: High levels of spatial and temporal variability shaped by nutrient availability and turbulence. *Scientific Reports, 7*(1), 6611. https://doi.org/10.1038/s41598-017-06928-z

Plähn, O., Baschek, B., Badewien, T. H., Walter, M., & Rhein, M. (2002). Importance of the Gulf of Aqaba for the formation of bottom water in the Red Sea. *Journal of Geophysical Research: Oceans, 107*(C8), 22.

Post, A. F., Dedej, Z., Gottlieb, R., Li, H., Thomas, D. N., El-Absawi, M., & Sommer, U. (2002). Spatial and temporal distribution of *Trichodesmium* spp. in the stratified Gulf of Aqaba, Red Sea. *Marine Ecology Progress Series, 239*, 241–250.

Post, A. F., Penno, S., Zandbank, K., Paytan, A., Huse, S. M., & Welch, D. M. (2011). Long term seasonal dynamics of Synechococcus population structure in the Gulf of Aqaba, Northern Red Sea. *Frontiers in Microbiology, 2*, 131.

Prabowo, D. A., & Agusti, S. (2019). Free-living dinoflagellates of the central Red Sea, Saudi Arabia: Variability, new records and potentially harmful species. *Marine Pollution Bulletin, 141*, 629–648. https://doi.org/10.1016/j.marpolbul.2019.03.012

Qurban, M. A., Balala, A. C., Kumar, S., Bhavya, P. S., & Wafar, M. (2014). Primary production in the northern Red Sea. *Journal of Marine Systems, 132*, 75–82. https://doi.org/10.1016/j.jmarsys.2014.01.006

Qurban, M. A., Wafar, M., Jyothibabu, R., & Manikandan, K. P. (2017). Patterns of primary production in the Red Sea. *Journal of Marine Systems, 169*, 87–98. https://doi.org/10.1016/j.jmarsys.2016.12.008

Racault, M. F., Raitsos, D. E., Berumen, M. L., Brewin, R. J., Platt, T., Sathyendranath, S., & Hoteit, I. (2015). Phytoplankton phenology indices in coral reef ecosystems: Application to ocean-color observations in the Red Sea. *Remote Sensing of Environment, 160*, 222–234. https://doi.org/10.1016/j.rse.2015.01.019

Raitsos, D. E., Pradhan, Y., Brewin, R. J., Stenchikov, G., & Hoteit, I. (2013). Remote sensing the phytoplankton seasonal succession of the Red Sea. *PLoS One1, 8*(6), Article e64909.

Rasul, N. M., Stewart, I. C., Vine, P., & Nawab, Z. A. (2018). Introduction to oceanographic and biological aspects of the Red Sea. In *Oceanographic and Biological Aspects of the Red Sea* (pp. 1–9). Cham: Springer International Publishing.

Reiss, Z., & Hottinger, L. (2012). *The Gulf of Aqaba: Ecological Micropaleontology* (Vol. 50). Springer Science & Business Media.

Şahin, F., Bat, L., Ediger, D., & Al-Najjar, T. (2022). Ecological and phytogeographical status and species composition of the phytoplankton in the Gulf of Aqaba (Red Sea). *Kahramanmaraş Sütçü İmam Üniversitesi Tarım Ve Doğa Dergisi, 25*(3), 606–616.

Sofianos, S. S., & Johns, W. E. (2003). An oceanic general circulation model (OGCM) investigation of the Red Sea circulation: 2. Three-dimensional circulation in the Red Sea. *Journal of Geophysical Research: Oceans, 108*(C3).

Sofianos, S. S., Johns, W. E., & Murray, S. P. (2002). Heat and freshwater budgets in the Red Sea from direct observations at Bab el Mandeb. *Deep Sea Research Part II: Topical Studies in Oceanography, 49*(7–8), 1323–1340.

Sommer, U. (2000). Scarcity of medium-sized phytoplankton in the northern Red Sea explained by strong bottom-up and weak top-down control. *Marine Ecology Progress Series, 197*, 19–25.

Sommer, U., Berninger, U. G., Böttger-Schnack, R., Cornils, A., Hagen, W., Hansen, T., & Wickham, S. (2002). Grazing during early spring in the Gulf of Aqaba and the northern Red Sea. *Marine Ecology Progress Series, 239*, 251–261.

Stambler, N. (2005). Bio-optical properties of the northern Red Sea and the Gulf of Eilat (Aqaba) during winter 1999. *Journal of Sea Research, 54*(3), 186–203.

Stambler, N. (2006). Light and picophytoplankton in the Gulf of Eilat (Aqaba). *Journal of Geophysical Research: Oceans, 111*(C11).

Taylor, F. J. R. (1976). Dinoflagellates from the International Indian Ocean Expedition. a material collected by the RV" Anton Bruun" 1963-1964. *BiblBot, 132*, 1–234.

Tomas, C. R. (1997). In *Identifying marine phytoplankton* (1st ed.). Academic Press.

Triantafyllou, G., Yao, F., Petihakis, G., Tsiaras, K. P., Raitsos, D. E., & Hoteit, I. (2014). Exploring the Red Sea seasonal ecosystem functioning using a three-dimensional biophysical model. *Journal of Geophysical Research: Oceans, 119*(3), 1791–1811. https://doi.org/10.1002/2013JC009641

Wafar, M., Qurban, M. A., Ashraf, M., Manikandan, K. P., Flandez, A. V., & Balala, A. C. (2016). Patterns of distribution of inorganic nutrients in Red Sea and their implications to primary production. *Journal of Marine Systems, 156*, 86–98. https://doi.org/10.1016/j.jmarsys.2015.12.003

Zhan, P., Subramanian, A. C., Yao, F., & Hoteit, I. (2014). Eddies in the Red Sea: A statistical and dynamical study. *Journal of Geophysical Research: Oceans, 119*(6), 3909–3925. https://doi.org/10.1002/2013JC009563